Journal Pre-proofs

The role of surface properties in the cathodoluminescence of Zn_2GeO_4/SnO_2 nanowire heterostructures

J. Dolado, P. Hidalgo, B. Méndez

PII: S0167-577X(20)30857-0
DOI: https://doi.org/10.1016/j.matlet.2020.128152
Reference: MLBLUE 128152

To appear in: *Materials Letters*

Revised Date: 9 June 2020
Accepted Date: 10 June 2020

Please cite this article as: J. Dolado, P. Hidalgo, B. Méndez, The role of surface properties in the cathodoluminescence of Zn_2GeO_4/SnO_2 nanowire heterostructures, *Materials Letters* (2020), doi: https://doi.org/10.1016/j.matlet.2020.128152

The role of surface properties in the cathodoluminescence of Zn_2GeO_4/SnO_2 nanowire heterostructures

J. Dolado, P. Hidalgo, B. Méndez

Departamento de Física de Materiales, Universidad Complutense de Madrid, E-28040 Madrid, Spain

Abstract

Herein, we report the influence of the surface conditions on the cathodoluminescence (CL) emissions from Zn_2GeO_4 nanowires and Zn_2GeO_4/SnO_2 heterostructures obtained by thermal evaporation technique. A Zn_2GeO_4 nanowire surrounded by a discontinuous shell of SnO_2 crystals composed the Zn_2GeO_4/SnO_2 heterostructures. Local CL measurements at different acceleration voltages allow monitoring the emission bands originated at the interface region, showing an additional deep-ultraviolet (UV) emission at 4.40 eV, which has not been previously reported. CL spectra from SnO_2 coated Zn_2GeO_4 nanowires also show this deep-UV emission. The results would confirm the presence of a shallow energy level close to the conduction band, which becomes active by passivation of Zn_2GeO_4 nanowires surface by the SnO_2 coating.

Keywords: `Zinc germanate, UV luminescence, nanowires.`

2010 MSC: 00-01, 99-00

1. Introduction

Ultra-wide bandgap semiconductors have emerged as promising functional materials in many applications due to their optoelectronic properties. In this sense, Zn_2GeO_4, $E_g \sim 4.5$ eV, is recently attracting a lot of interest for showing

*Corresponding author
Email address: `jdolado@ucm.es` (J. Dolado)

acceptable electronic conductivity while keeping optical transparency up to the ultraviolet (UV) range [1]. Regarding the optical properties, oxygen vacancies and zinc interstitials in Zn_2GeO_4 microwires have been recently proposed as responsible centers for emission bands in the visible and in the UV region at 3.45 eV [2, 3]. However, the origin of these emissions is still uncertain and factors, as the role of the surface in Zn_2GeO_4 nanowires, have not yet been explored. Herein, we have fabricated single and complex Zn_2GeO_4 nanowires by thermal evaporation technique. In particular, Zn_2GeO_4/SnO_2 heterostructures with a skewer-like arrangement, consisting of a central Zn_2GeO_4 nanowire surrounded by a discontinuous shell of SnO_2 crystallites have been prepared [4]. This self-assembled heterostructure is a very suitable system to assess the eventual role that surface states could play in the UV emissions of Zn_2GeO_4 nanowires due to band bending effects at the interface.

In this work, local CL measurements from the Zn_2GeO_4/SnO_2 heterostructures recorded at increasing acceleration voltages of the electron beam have been performed. The CL data have been discussed in the light of the Monte Carlo simulations (MCs) of the electron de-excitation paths. Besides the visible and UV bands reported from Zn_2GeO_4 and SnO_2 attributed to native defects, an additional deep-UV emission at 4.40 eV is eventually detected, not observed in Zn_2GeO_4 bare material. Comparatively, Zn_2GeO_4 wires coated with a SnO_2 thin layer have been prepared and the CL results also show the deep-UV component. The results support the conclusion that a shallow level near the conduction band in Zn_2GeO_4 is activated by the heterostructure formation.

2. Experimental methods

The synthesis of the Zn_2GeO_4 nanowires and heterostructures was carried out by thermal evaporation. A mixture of ZnO:Ge:C powders (2:1:2 wt %) and SnO_2 in 10% wt of Zn:Ge was conducted during 8 h at 800 ^{o}C under an Ar flow of 1.5 l/min [4]. Samples were transferred to a silicon wafer for characterization. For comparison, Zn_2GeO_4 nanowires coated with a thin SnO_2

layer by means of a Quorum Technologies Q-150-T ES Plus automatic sputter coater were also studied. The structural characterization has been performed by Raman spectroscopy in a Horiba-Jobin-Ybon optical confocal microscope using a 325 nm He-Cd laser. The morphology and CL spectra have been carried out by using a FEI Inspect scanning electron microscope (SEM) and a Hitachi S-2500 SEM equipped with a PMA-12 charge coupled device camera for CL measurements.

3. Results and discussion

Figure 1a shows a SEM image of the Zn_2GeO_4/SnO_2 heterostructures that are composed of a Zn_2GeO_4 axis (100-200 nm wide) in which SnO_2 crystals are inserted along. Local Raman spectra at the points marked by arrows in the inset of Figure 1b have been recorded to check the microstructure. Figure 1b shows Raman peaks representative of the rutile phase of SnO_2 corresponding to the E_g (478 cm^{-1}), A_{1g} (634 cm^{-1}) and B_{2g} (778 cm^{-1}) vibration modes [5]. On the other hand, figure 1c shows the characteristic Raman peaks of the rhombohedral structure of Zn_2GeO_4 (745, 751, 777 and 802 cm^{-1}) associated with Ge-O-Zn symmetric and asymmetric vibration modes and the O-Ge-O bending and stretching modes [6, 7]. The 520 cm^{-1} peak corresponds to the silicon substrate.

In order to assess the electronic levels in a non-destructive way with z-resolution, we have carried out CL spectra of the Zn_2GeO_4/SnO_2 heterostructures at increasing acceleration voltages (V_{acc}) of the electron beam. Besides, the CASINO software based on Monte Carlo calculations [8] has been used to simulate the penetration profiles of the electrons and to calculate the CL signal generation volume. The results of these simulations are shown in Figure 2. The Zn_2GeO_4 and SnO_2 transversal sizes have been measured from the SE image of the inset in Figure 1b and helped to sketch the heterostructure (Figure 2a). The rate of the CL intensity recorded for 5 kV $< V_{acc} <$ 12 kV is plotted in Figures 2c-d, and show that the highest percentage of CL emission comes from

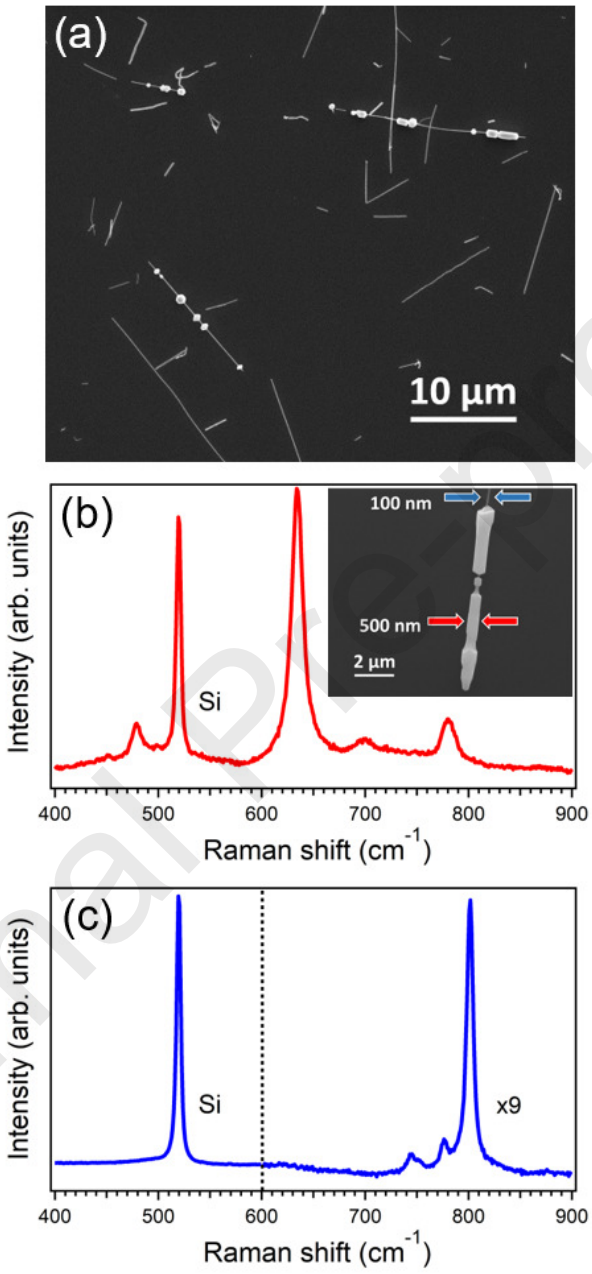

Figure 1: (a) SE image of Zn_2GeO_4/SnO_2 heterostructures and Zn_2GeO_4 nanowires deposited onto a silicon wafer. Raman spectra acquired from the SnO_2 coating (b), and from the Zn_2GeO_4 nanowire (c). Inset in (b): SE image of the studied heterostructure.

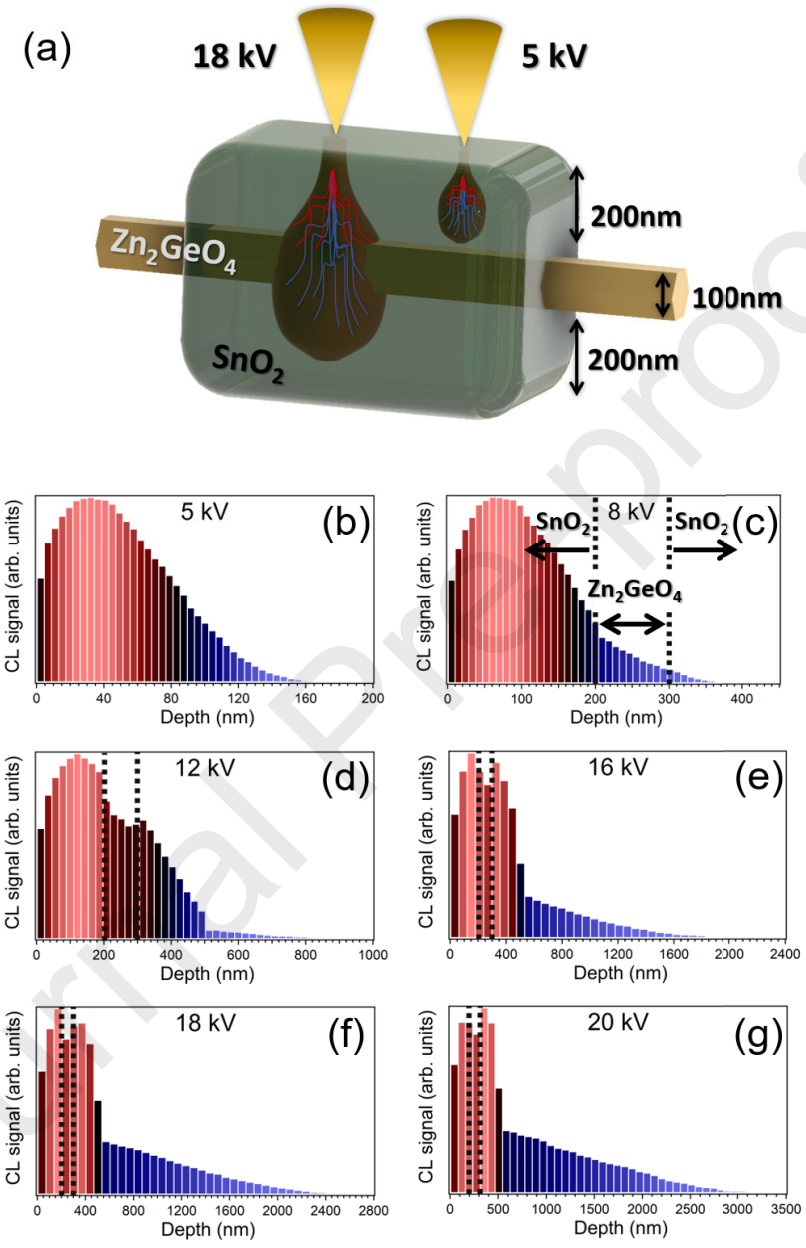

Figure 2: (a) Sketch of the heterostructure. (b)-(g) Rate of CL intensity as a function of sample depth for increasing V_{acc}. Vertical dotted lines are used to locate the central Zn_2GeO_4 nanowire.

the SnO_2 crystallite (area outside the dashed lines). On the other hand, the simulation shows that for $V_{acc} > 12$ kV (Figures 2e-g) the signal is generated in through the whole Zn_2GeO_4/SnO_2 assembly including the interface region.

Figure 3a shows the CL spectra recorded on the point indicated by red arrows in Figure 1b (inset) for 5 kV $< V_{acc} <$ 20 kV. For the sake of clarity, normalized CL spectra are plotted in Figure 3b. The dominant emission at 2.1-2.4 eV is attributed to native defects in SnO_2, which shows characteristic bands in this range [9]. In particular, for 5 kV $< V_{acc} <$ 12 kV, the CL spectra only displays this broad band. For $V_{acc} > 16$ kV, the electron beam goes deeper in the sample and reaches the Zn_2GeO_4 nanowire, which could lead to additional emission bands. In particular, photoluminescence and CL studies of Zn_2GeO_4 microrods have reported bands in the visible (2.3 eV) and in the UV (3.45 eV) generally attributed to intrinsic point defects involving oxygen vacancies and/or zinc interstitials as donor levels and cation vacancies as acceptor levels [2, 3, 10]. Here, the CL spectra for $V_{acc} > 16$ kV show an increase of the CL intensity in the UV region that could be related to the UV band of Zn_2GeO_4 along with an additional emission peaked at 4.40 eV. Taking into account the MCs, we suggest that this deep-UV emission could be related to the influence of SnO_2 on the surface states of Zn_2GeO_4, leading to the activation of shallow energy levels linked to the oxygen vacancies states. The band bending effects and the formation of a shallow depletion region at the oxides surface as a consequence of oxygen exchange have been reported in TiO_2 or Zn_2GeO_4 nanowires [11, 12].

Finally, to verify the role of SnO_2 in this deep-UV emission and elucidate its effect on the Zn_2GeO_4 surface electronic properties, a 20 nm Sn thin layer was deposited by sputtering on Zn_2GeO_4 nanowires (Figure 3c), which turned into SnO_2 under ambient conditions. Figure 3d (red line) shows the CL spectrum of the as-grown Zn_2GeO_4 nanowires with the UV band at around 3.45 eV related to oxygen vacancies in this ternary oxide [3]. However, the CL spectrum recorded after Sn deposition and oxidation (blue line in Figure 3d) shows, although weak, the band around 4.40 eV above observed. It should be noticed that the layer of SnO_2 in this case is very thin in comparison with the SnO_2 crystallites in the

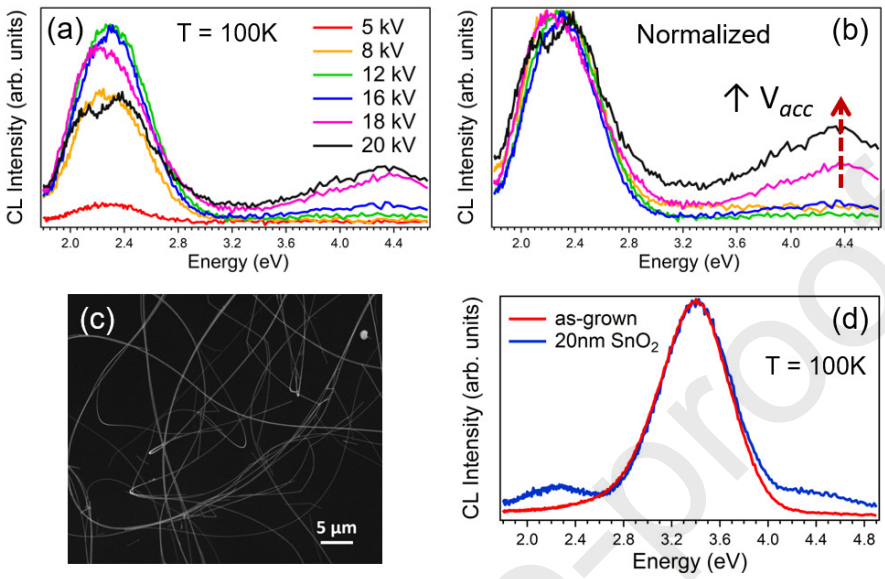

Figure 3: (a-b) Local CL spectra from a Zn_2GeO_4/SnO_2 heterostructure for different V_{acc}. (c) SE image of Zn_2GeO_4 nanowires. (d) CL spectra acquired at 15 kV from as-grown Zn_2GeO_4 nanowires (red line) and after 20 nm SnO_2 deposition (blue line).

heterostructures, and hence the visible emission related to SnO_2 is weak. The appearance of the deep-UV band would confirm the need of some coating of the Zn_2GeO_4 nanowires to achieve radiative recombination from shallow levels to the valence band, which otherwise are not active. This process could be possible by Zn_2GeO_4 band bending effects at the Zn_2GeO_4/SnO_2 interface. The results would be of interest in applications for solar cells, where the surface passivation is a key factor to significantly improve some relevant parameters in the device performance [13]. Future studies will be carried out in order to gain more knowledge about the surface states related bands in Zn_2GeO_4.

4. Conclusions

The UV luminescence of SnO_2 coated Zn_2GeO_4 nanowires have been studied. The CL results show the UV and visible bands reported from Zn_2GeO_4 and SnO_2, respectively, attributed to native defects. However, local CL measure-

ments in Zn_2GeO_4/SnO_2 nanowire heterostructures reveal a novel component at 4.40 eV originated at the interface region, as the MCs data would confirm. In order to check the role of the SnO_2, CL spectra from bare and Zn_2GeO_4 wires coated with a SnO_2 thin layer were also carried out. The main luminescence band is centered at 3.45 eV, but the deep-UV band at 4.40 eV only appears in coated nanowires. The results support that a shallow level near the conduction band in Zn_2GeO_4 is activated by passivation of Zn_2GeO_4 nanowires surface by the SnO_2 coating.

5. Acknowledgement

This work was supported by MICIN (Grant RTI2018-09195-B-I00).

References

[1] H. Mizoguchi, T. Kamiya, S. Matsuishi, H. Hosono, A germanate transparent conductive oxide, Nat. Commun. 2 (1) (2011) 470.

[2] L. Liu, X. Zhao, H. Sun, C. Jia, W. Fan, Theoretical study of H_2O adsorption on Zn_2GeO_4 surfaces: Effects of surface state and structure–activity relationships, ACS Appl. Mater. Interfaces 5 (15) (2013) 6893 – 6901.

[3] P. Hidalgo, A. López, B. Méndez, J. Piqueras, Synthesis and optical properties of Zn_2GeO_4 microrods, Acta Materialia 104 (2016) 84 – 90.

[4] J. Dolado, K. L. Renforth, J. E. Nunn, S. A. Hindsmarsh, P. Hidalgo, A. M. Sánchez, B. Méndez, Zn_2GeO_4/SnO_2 Nanowire heterostructures driven by Plateau–Rayleigh instability, Crystal Growth & Design 20 (1) (2020) 506–513.

[5] S. Sun, G. Meng, G. Zhang, T. Gao, B. Geng, L. Zhang, J. Zuo, Raman scattering study of rutile SnO_2 nanobelts synthesized by thermal evaporation of Sn powders, Chemical Physics Letters 376 (1) (2003) 103 – 107.

[6] J. Dolado, P. Hidalgo, B. Méndez, Correlative study of vibrational and luminescence properties of Zn_2GeO_4 microrods, physica status solidi (a) 215 (19) (2018) 1800270.

[7] Y. Zhao, S. Yang, J. Zhu, G. Ji, F. Peng, The study of oxygen ion motion in Zn_2GeO_4 by Raman spectroscopy, Solid State Ionics 274 (2015) 12 – 16.

[8] D. Drouin, A. R. Couture, D. Joly, X. Tastet, V. Aimez, R. Gauvin, Casino v2.42—a fast and easy-to-use modeling tool for scanning electron microscopy and microanalysis users, Scanning 29 (3) (2007) 92–101.

[9] D. Maestre, A. Cremades, J. Piqueras, Cathodoluminescence of defects in sintered tin oxide, Journal of Applied Physics 95 (6) (2004) 3027–3030.

[10] V.-H. Pham, V. T. Kien, P. D. Tam, P. T. Huy, Luminescence of one dimensional ZnO, GeO_2 - Zn_2GeO_4 nanostructure through thermal evaporation of Zn and Ge powder mixture, Materials Science and Engineering: B 209 (2016) 17 – 22.

[11] G. Mattioli, F. Filippone, P. Alippi, A. Amore Bonapasta, Ab initio study of the electronic states induced by oxygen vacancies in rutile and anatase TiO_2, Phys. Rev. B (2008) 241201.

[12] C.-H. Liao, C.-W. Huang, J.-Y. Chen, C.-H. Chiu, T. Tsai, K.-C. Lu, M.-Y. Lu, W.-W. Wu, Optoelectronic properties of single-crystalline Zn_2GeO_4 nanowires, The Journal of Physical Chemistry C 118 (15) (2014) 8194–8199.

[13] J. Yu, M. Liao, D. Yan, Y. Wan, H. Lin, Z. Wang, P. Gao, Y. Zeng, B. Yan, J. Ye, Activating and optimizing evaporation-processed magnesium oxide passivating contact for silicon solar cells, Nano Energy 62 (2019) 181 – 188.